

Michael Kruse,<sup>1,2,3</sup> Farnaz Keyhani-Nejad,<sup>1,2,3</sup> Frank Isken,<sup>1,2,3</sup> Barbara Nitz,<sup>3,4,5</sup>  
 Anja Kretschmer,<sup>4,5</sup> Eva Reischl,<sup>4,5</sup> Tonia de las Heras Gala,<sup>5</sup> Martin A. Osterhoff,<sup>1,2,3</sup>  
 Harald Grallert,<sup>3,4,5</sup> and Andreas F.H. Pfeiffer<sup>1,2,3</sup>



## High-Fat Diet During Mouse Pregnancy and Lactation Targets GIP-Regulated Metabolic Pathways in Adult Male Offspring

Diabetes 2016;65:574–584 | DOI: 10.2337/db15-0478

**Maternal obesity is a worldwide problem associated with increased risk of metabolic diseases in the offspring. Genetic deletion of the gastric inhibitory polypeptide (GIP) receptor (GIPR) prevents high-fat diet (HFD)-induced obesity in mice due to specific changes in energy and fat cell metabolism. We investigated whether GIP-associated pathways may be targeted by fetal programming and mimicked the situation by exposing pregnant mice to control or HFD during pregnancy (intrauterine [IU]) and lactation (L). Male wild-type (WT) and *Gipr*<sup>-/-</sup> offspring received control chow until 25 weeks of age followed by 20 weeks of HFD. *Gipr*<sup>-/-</sup> offspring of mice exposed to HFD during IU/L became insulin resistant and obese and exhibited increased adipose tissue inflammation and decreased peripheral tissue substrate utilization after being reintroduced to HFD, similar to WT mice on regular chow during IU/L. They showed decreased hypothalamic insulin sensitivity compared with *Gipr*<sup>-/-</sup> mice on control diet during IU/L. DNA methylation analysis revealed increased methylation of CpG dinucleotides and differential transcription factor binding of promoter regions of genes involved in lipid oxidation in the muscle of *Gipr*<sup>-/-</sup> offspring on HFD during IU/L, which were inversely correlated with gene expression levels. Our data identify GIP-regulated metabolic pathways that are targeted by fetal programming.**

Gastric inhibitory polypeptide (GIP) is released from the duodenum after nutrient intake and regulates postprandial

insulin secretion (1). GIP is known for its anabolic effects in adipocytes (2) and has been shown to stimulate the activity of lipoprotein lipase in adipose tissue in vitro (3) (4). Genetic ablation of the GIP receptor (GIPR) protects from high-fat diet (HFD)-induced obesity and insulin resistance in mice (5). GIPR knockout (*Gipr*<sup>-/-</sup>) mice use fat as energy substrate rather than storing it in adipocytes. Moreover, central appetite-regulating pathways are down-regulated in ovariectomized female *Gipr*<sup>-/-</sup> mice (6), and energy expenditure is increased in *Gipr*<sup>-/-</sup> mice exposed to a high-glycemic index diet (7) or an HFD (8).

Since *Gipr*<sup>-/-</sup> mice are protected from obesity when exposed to a postweaning HFD, we hypothesized that this phenotype may be lost when these mice were exposed to the same HFD during pregnancy (intrauterine [IU]) and lactation (L). The IU milieu has a persisting influence on the development of adult diseases (9,10). Maternal caloric malnutrition as well as overnutrition during IU and L can induce metabolic disturbances later in life in offspring (11,12). Animal studies have shown that mice exposed to a maternal HFD during IU/L and weaned onto a standard chow developed adiposity, insulin resistance, and hepatosteatosis later in life (13,14). Not only the diet during IU/L but also the postweaning diet is important for the manifestation of metabolic diseases. Studies investigating the interaction of an HFD during IU/L and postweaning usually apply the HFD continuously from preweaning throughout the end of the study in adulthood.

<sup>1</sup>Department of Clinical Nutrition, German Institute of Human Nutrition, Nuthetal, Germany

<sup>2</sup>Department of Endocrinology and Metabolic Diseases, Charité–University of Medicine, Berlin, Germany

<sup>3</sup>German Center for Diabetes Research, Neuherberg, Germany

<sup>4</sup>Research Unit of Molecular Epidemiology, German Research Center for Environmental Health, Helmholtz Zentrum München, Neuherberg, Germany

<sup>5</sup>Institute of Epidemiology II, German Research Center for Environmental Health, Helmholtz Zentrum München, Neuherberg, Germany

Corresponding author: Andreas F.H. Pfeiffer, afhp@dife.de.

Received 8 April 2015 and accepted 20 November 2015.

This article contains Supplementary Data online at <http://diabetes.diabetesjournals.org/lookup/suppl/doi:10.2337/db15-0478/-/DC1>.

M.K. and F.K.-N. contributed equally to this work.

© 2016 by the American Diabetes Association. Readers may use this article as long as the work is properly cited, the use is educational and not for profit, and the work is not altered.

However, in terms of programming effects of metabolic diseases, studies investigating a “second hit” later in life (e.g., a HFD) after a time frame of regular diet might better reflect the adult onset of obesity, as shown recently (15). Recent work suggests that the IU milieu induces epigenetic alterations, such as DNA methylation and histone modifications, which affect gene transcription that persists throughout life (16). Pathways targeted by epigenetic programming are of eminent importance to develop strategies to reduce the metabolic risks faced by offspring of obese mothers. We therefore chose a model in which extensive research has already identified some pathways involved in the protection from obesity, the *Gipr*<sup>-/-</sup> mouse.

Our results demonstrate that *Gipr*<sup>-/-</sup> mice exposed to an HFD during IU/L, weaned onto a regular chow for 22 weeks, and then reexposed to the HFD lose their metabolic protection, which is associated with hypermethylation of certain CpG dinucleotides in the promoter regions of genes involved in energy balance and with changes in central insulin sensitivity. This phenotype was similar to wild-type (WT) mice that were exposed to a control chow during IU/L but also challenged with an HFD later in life. We therefore conclude that the protection from diet-induced obesity in *Gipr*<sup>-/-</sup> mice is “overruled” by deleterious and persistent fetal programming effects of an HFD up to at least 45 weeks of life and identify metabolic pathways addressed by GIP.

## RESEARCH DESIGN AND METHODS

### Animals and Experimental Design

Animals were maintained on a 12-h light-dark cycle with ad libitum access to chow and water. Age- and body weight-matched female mice heterozygote for the GIPR (*Gipr*<sup>+/-</sup>) on a C57BL/6 background were maintained on

either a control (C) diet D12450B (10% kcal fat as soybean oil and lard, 20% kcal protein, 70% kcal carbohydrate, 3.85 kcal/g) or an HFD D12492 (60% kcal fat as soybean oil and lard, 20% kcal protein, 20% kcal carbohydrate, 5.24 kcal/g) 2 weeks prior to mating with a male *Gipr*<sup>+/-</sup> mouse and throughout IU and L (all diets from Research Diets, Inc., New Brunswick, NJ). Offspring were genotyped at 2–3 weeks of life. Male *Gipr*<sup>-/-</sup> offspring on C diet or HFD during IU/L and WT offspring on C diet during IU/L were individually housed and placed onto C diet at postnatal day 21 and kept on this diet until the age of 25 weeks, followed by a further 20 weeks on HFD. This resulted in *Gipr*<sup>-/-</sup> mice exposed to C diet during IU/L and to HFD at the age of 25 weeks (KO C-C-H), *Gipr*<sup>-/-</sup> mice exposed to HFD during IU/L and to HFD at the age of 25 weeks (KO H-C-H), and WT mice exposed to C diet during IU/L and to HFD at the age of 25 weeks (WT C-C-H). Results obtained for these groups during the first 25 weeks of life are indicated with the first two diet symbols (KO C-C, KO H-C, and WT C-C). At the age of 45 weeks, mice were killed using cervical dislocation. Tissues were harvested, immediately frozen in liquid nitrogen, and stored at -80°C. Figure 1 illustrates the study design. Animal protocols were approved by the local governmental animal ethic review board (State of Brandenburg).

### Biochemical Measurements

Fasting blood samples were collected after an overnight fast at 45 weeks of age from the submandibular vein plexus. Serum glucose, triglycerides, total cholesterol, and nonesterified fatty acids (NEFAs) were measured using commercial kits (glucose HK 125, ABX Diagnostics, Montpellier, France; triglycerides and total cholesterol, ABX Pentra, Montpellier, France; and NEFA HR, Wako Chemicals, Neuss, Germany) by using an autoanalyzer

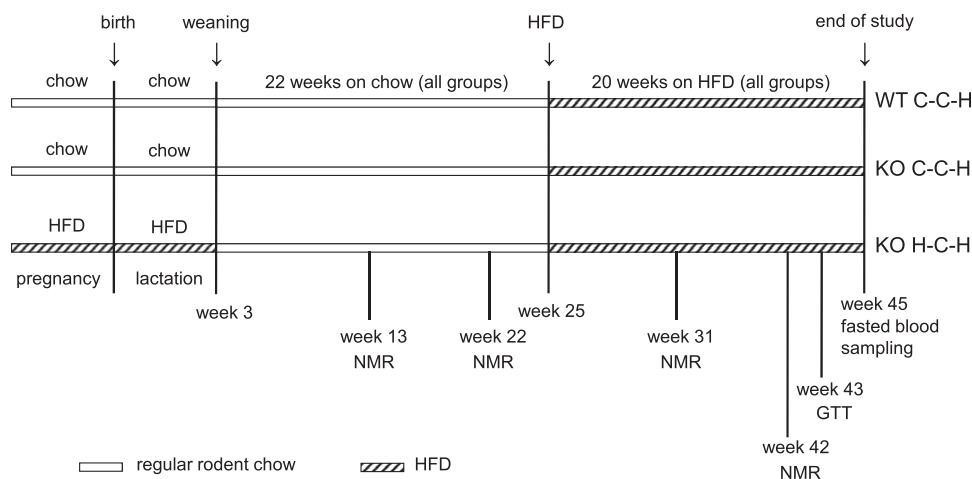


**Figure 1**—Schematic representation of the study. Exposure to either a C diet or an HFD (H) during pregnancy and lactation results in three different experimental groups (WT C-C-H, KO C-C-H, and KO H-C-H): the first letter indicates the diet during pregnancy and lactation, the second letter indicates the diet postweaning up to the age of 25 weeks, and the third letter indicates the diet during the last 20 weeks of life (until the age of 45 weeks). GTT, intraperitoneal GTT; KO, *Gipr*<sup>-/-</sup> offspring; NMR, nuclear MRS.

(Cobas Mira S, Hoffmann-La Roche, Basel, Switzerland). Plasma insulin levels were determined as previously described (17).

#### **Body Weight and Cumulative Food Intake**

Body weight and cumulative food intake were measured weekly. Food consumption was expressed in kilocalories per gram of body weight for the indicated age.

#### **Intraperitoneal Glucose Tolerance Test**

A glucose tolerance test (GTT) was performed at the age of 43 weeks. Overnight-fasted mice received an injection of D-(+)-glucose (2.0 g/kg body wt i.p.) (18). Blood was taken from the submandibular vein plexus and added to heparinized collecting tubes for plasma glucose and insulin measurements at 0, 10, 30, 60, and 120 min after glucose injection.

#### **Body Composition**

Body composition was determined by nuclear MRS (minispect MQ 10 NMR Analyzer; Bruker, Karlsruhe, Germany) in conscious mice (6) at the age of 13, 22, 31, and 42 weeks of life.

#### **Quantitative Real-Time PCR Analysis**

mRNA expression was performed in epididymal white adipose tissue, gastrocnemius muscle, and hypothalamus as previously described (6,19). The hypothalamus was dissected as a whole without any further subfractionation. Primers were designed using Primer Express software (Applied Biosystems). Primer sequences are listed in Supplementary Table 1. The constitutive gene HPRT was used as a housekeeping gene.

#### **Hypothalamic Insulin Signaling**

The hypothalamic insulin signaling pathway was analyzed by performing the PathScan Intracellular Signaling Array Kit (Cell Signaling Technology, Danvers, MA) that allows a quantitative analysis of the phosphorylation status of key proteins involved in insulin and energy signaling. Total protein lysate (75  $\mu$ L) was processed following the manufacturer's instructions. Signal density was visualized using LI-COR Biosciences Odyssey (LI-COR Bioscience, Bad Homburg, Germany).

#### **Histology of White Adipose Tissue**

Tissue was fixed in 10% buffered formalin, embedded in paraffin, sectioned at 5  $\mu$ m, and stained with hematoxylin-eosin. Adipocyte size was measured using CellProfiler 2.0 ([www.cellprofiler.org](http://www.cellprofiler.org)). One visual field with at least 40 cells of three samples of epididymal adipose tissue from one animal was analyzed for cell surface size and expressed in micrometers squared. The average adipocyte cell size for each group was calculated, and the frequency of cell sizes sorted by categories was determined for each group.

For evaluation of crown-like structures, 2- $\mu$ m sections were dewaxed using 3% hydrogen peroxide and incubated overnight (4°C) with an F4/80 anti-mouse antibody (1:8,000; Serotec, Puchheim, Germany), followed by an

anti-rat secondary antibody for mouse tissue that includes Histofine (Nichirei Biosciences Inc., Tokyo, Japan). Images were acquired by Mirax slide scanner (Carl Zeiss, Göttingen, Germany). Crown-like structures were determined in three randomly chosen areas within the slides.

#### **DNA Methylation Analysis**

##### **DNA Extraction**

Genomic DNA was extracted from muscle and hypothalamus using a commercial kit (Machery-Nagel, Dueren, Germany) following the manufacturer's protocol, and quality was checked using a NanoDrop ND-1000 Spectrophotometer (PEQLAB, Erlangen, Germany).

##### **Sodium Bisulfite Modification**

Genomic DNA (700–1,000 ng) was bisulfite treated using the EZ-96 DNA Methylation Kit (Zymo Research, Orange, CA) according to the manufacturer's protocol.

##### **DNA Methylation Analysis by Mass Spectrometry**

Methylation was determined for five loci by MALDI-TOF (matrix-assisted laser desorption ionization time-of-flight) mass spectrometry using EpiTYPER by MassARRAY (Sequenom, San Diego, CA) as previously described (20,21). Briefly, the target regions were amplified from bisulfite-treated DNA in duplicate PCR reactions. Primers were designed using the Sequenom EpiDesigner Web resource (<http://www.epidesigner.com>). Primer sequences for all amplicons are listed in Supplementary Table 2. Methylation data were generated by the MassARRAY EpiTYPER v1.2 software (Sequenom).

Four samples were measured in duplicate for four amplicons. Quality control of the data was performed using EpiTyper and the statistical software R (version 3.0.2), eliminating all samples and all CpG sites with a call rate <80%, respectively. In total, 182 CpG dinucleotides were measured (single sites and composite sites with two or more adjacent CpG sites falling within one analyzed fragment). CpG dinucleotides relevant for this study are named regarding their distance to the transcription start site.

##### **Electrophoretic Mobility Shift Assays**

Myoblast nuclear extracts from mouse C2C12 cells (no. 36078; Active Motif) were used for electrophoretic mobility shift assay (EMSA). Cy5-labeled and unlabeled oligonucleotides (Metabion) containing the methylated or unmethylated CpG from respective EpiTYPER experiments (Supplementary Table 3) were annealed and purified in a 12% polyacrylamide gel. Binding reaction was carried out with or without different concentrations of unlabeled competitor oligonucleotides. In each reaction, 6.5  $\mu$ g nuclear extract was incubated in 5 $\times$  binding buffer (4% vol/vol glycerol, 1 mmol/L MgCl<sub>2</sub>, 0.5 mmol/L EDTA, 0.5 mmol/L dithiothreitol, 50 mmol/L NaCl, and 10 mmol/L Tris HCl, pH 7.5) with 0.5  $\mu$ g Poly[d(I-C)] (Roche Diagnostics) and 1 ng labeled probe in a total volume of 10  $\mu$ L for 25 min at 4°C. Protein-DNA complexes were

separated on a 5.3% polyacrylamide gel by electrophoresis in 0.5× trisborate EDTA running buffer. The gels were visualized by scanning with the Trio Typhoon plus Typhoon imager (GE Healthcare).

**Data Analysis**

Data are represented as means ± SEM. Statistical analyses were performed using one-way ANOVA with Tukey post hoc test (version 20; SPSS, Chicago, IL). Data were tested for normal distribution. Non-normally distributed data were transformed to the logarithmic form to approximate the normal distribution.

Statistical analysis on methylation data was performed using R (version 3.0.2). For DNA methylation analysis, inferential statistics was used to analyze the 182 CpG sites of the three groups. For inferential statistics, Student *t* test

was performed and resulting *P* values were adjusted for multiple testing. For descriptive analysis, quotients of mean values from each two groups were calculated. For verification we also performed a correlation analysis of methylation data and gene expression data.

**RESULTS**

**Body Weight, Body Composition, Food Intake, and Serum Lipids**

During the first 25 weeks of life, body weight was not different except for weeks 4, 13, and 14, when KO H-C was heavier than KO C-C (Fig. 2A). When an HFD was fed at week 25 of life, KO C-C-H showed a significantly lower increase in body weight than WT C-C-H (Fig. 2B). Body weight of KO H-C-H was in between the range of WT C-C-H and KO C-C-H. Before exposure to the HFD,

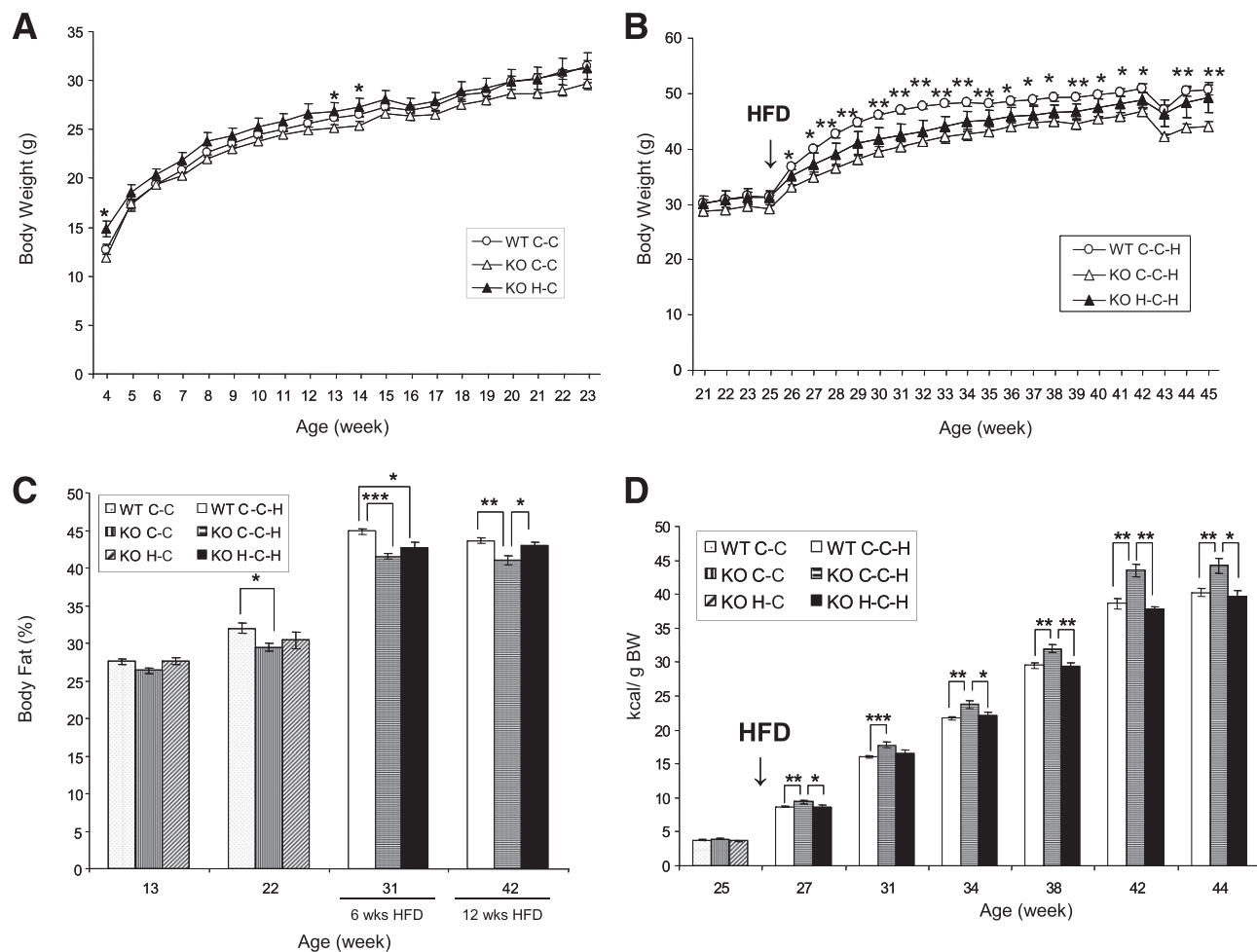


**Figure 2**—Body weight, adiposity, and energy intake. *A*: Growth curve of offspring from 4 weeks until 23 weeks of age on a standard rodent chow. Except for weeks 4, 13, and 14, there was no significant difference in body weight. \**P* < 0.05 for KO H-C compared with KO C-C. *B*: Growth curve of offspring after an HFD was started at 25 weeks of age. WT C-C-H gained significantly more weight compared with KO C-C-H. Body weight of KO H-C-H is in range between the two other groups. *C*: Adiposity was measured by nuclear MRS. KO H-C-H had significantly increased body fat compared with KO C-C-H after 12 weeks (wks) on an HFD, and KO C-C-H had significantly lower body fat compared with WT C-C-H. *D*: Cumulative energy intake is shown for selected time points. After an HFD was fed, WT C-C-H and KO H-C-H had similar cumulative food intake, which was lower compared with KO C-C-H. BW, body weight. \**P* < 0.05, \*\**P* < 0.01, \*\*\**P* < 0.005; *n* = 4–13 per group.

adiposity of KO C-C was significantly lower compared with WT C-C (Fig. 2C). After 12 weeks on the HFD, KO C-C-H showed a significant decrease in adiposity compared with WT C-C-H, but now KO H-C-H had significantly increased adiposity compared with KO C-C-H, similar to WT C-C-H.

When offspring were on a regular diet, there was no difference in cumulative food intake for all groups at the age of 25 weeks (Fig. 2D). When mice were fed an HFD, KO C-C-H consumed significantly more kilocalories per grams of body weight than WT C-C-H. In KO H-C-H, there was a significant decrease in cumulative energy consumption compared with KO C-C-H, which was similar to the level of WT C-C-H. Despite increased food intake, KO C-C-H had significantly reduced serum levels for total cholesterol compared with WT C-C-H ( $3.33 \pm 0.33$  vs.  $5.22 \pm 0.26$  mmol/L, respectively;  $P < 0.005$ ) (Table 1). In KO H-C-H, total cholesterol levels were  $4.44 \pm 0.40$  mmol/L, but this level was not significantly different compared with KO C-C-H. Serum levels for triglycerides and NEFA were unchanged.

#### KO H-C-H Mice Have Decreased Glucose Tolerance

The intraperitoneal GTT after 18 weeks on HFD showed that KO C-C-H had significantly lower fasting blood glucose levels compared with WT C-C-H (Fig. 3A and Table 1). However, KO H-C-H showed significantly increased fasting blood glucose levels compared with KO C-C-H ( $P < 0.05$ ), reaching levels similar to those of WT C-C-H. Accordingly, KO C-C-H had significantly lower fasting insulin levels compared with WT C-C-H ( $P < 0.05$ ) (Table 1). KO H-C-H showed severe glucose intolerance similar to WT C-C-H (Fig. 3A). KO C-C-H, however, had significantly lower glucose levels after 30 min ( $P < 0.05$  and  $P < 0.005$  compared with KO H-C-H and WT C-C-H, respectively) and after 90 min ( $P < 0.05$  compared with KO H-C-H and WT C-C-H). Additionally, the area under the curve for glucose (Fig. 3B) was lower in KO C-C-H compared with WT C-C-H ( $P < 0.05$ ) but increased again in KO H-C-H ( $P < 0.05$  compared with KO C-C-H, and  $P =$  not significant compared with WT C-C-H). During the intraperitoneal GTT, *Gipr*<sup>-/-</sup> mice showed slightly lower insulin levels compared with WT, with no significant difference between KO C-C-H and KO H-C-H (Fig. 3C and D).

#### Increased Adipocyte Size in KO H-C-H Mice

KO C-C-H had significantly smaller adipocytes compared with WT C-C-H ( $P < 0.001$ ) (Fig. 4A, C, and D). HFD during IU/L caused an increase in adipocyte size in KO H-C-H ( $P < 0.001$  compared with KO C-C-H) (Fig. 4A, D, and E). Figure 4B shows that KO C-C-H had more small adipocytes ( $<2,000 \mu\text{m}^2$ ) compared with KO H-C-H and WT C-C-H, which both had more cell counts in categories with large adipocytes ( $\geq 8,000 \mu\text{m}^2$ ).

#### KO H-C-H Mice Exhibit Increased Markers of Macrophage Infiltration in White Adipose Tissue

*Ccl2* mRNA expression was 48% decreased in KO C-C-H compared with WT C-C-H mice ( $P < 0.05$ ) (Fig. 5A). However, in KO H-C-H, *Ccl2* mRNA expression was increased 2.73-fold compared with KO C-C-H ( $P < 0.05$ ). *Ccl3* mRNA levels were significantly downregulated by 43% in KO C-C-H ( $P < 0.05$  compared with WT C-C-H) and again 1.39-fold upregulated in KO H-C-H compared with KO C-C-H; however, the difference was not significant. The same pattern was observed for mRNA expression of *Emr1*: it was decreased by 44% in KO C-C-H compared with WT C-C-H ( $P < 0.05$ ) and 1.35-fold upregulated in KO H-C-H ( $P =$  not significant compared with KO H-C-H). However, we could not detect differences in crown-like structures (Supplementary Fig. 1). There was no difference in gene expression for *Tnf* and *Il6*.

#### KO H-C-H Mice Show a Strong Decrease of Key Genes of Fatty Acid Oxidation in Muscle Compared with KO C-C-H Mice

A strong increase in gene expression levels of *Ppara* (2.45-fold,  $P < 0.01$ ), *Ppargc1a* (1.78-fold,  $P < 0.01$ ), *Cpt1a* (1.39-fold,  $P < 0.05$ ), and *Cpt1b* (1.53-fold,  $P < 0.01$ ) was observed in KO C-C-H compared with WT C-C-H (Fig. 5B). This increase was abolished when *Gipr*<sup>-/-</sup> mice were exposed to an HFD during IU/L (KO H-C-H). These mice had the same gene expression levels as WT C-C-H. We did not observe any significant difference in gene expression for *Cd36*, *Lpl*, *Acadm*, and *Acadl*.

#### Increased Gene Expression of Phosphatidylinositol 3-Kinase Regulatory Subunit p85 $\alpha$ in the Hypothalamus in KO H-C-H Mice

Hypothalamic gene expression of phosphatidylinositol 3-kinase (PI3K)-p85 $\alpha$  (*Pik3r1*) was 22% downregulated

**Table 1—Fasted glucose, insulin, total cholesterol, triglyceride, and NEFA serum levels at 45 weeks of age (20 weeks on HFD)**

	WT C-C-H	KO C-C-H	KO H-C-H
Blood glucose (mg/dL)	167 $\pm$ 9	118 $\pm$ 12¶,\$	160 $\pm$ 11
Insulin (ng/mL)	4.28 $\pm$ 0.32	2.17 $\pm$ 0.21*	3.58 $\pm$ 0.64
Cholesterol (mmol/L)	5.22 $\pm$ 0.26	3.33 $\pm$ 0.33§	4.44 $\pm$ 0.40
Triglycerides (mmol/L)	0.98 $\pm$ 0.04	0.88 $\pm$ 0.08	0.92 $\pm$ 0.04
NEFA (mmol/L)	0.86 $\pm$ 0.03	0.86 $\pm$ 0.06	0.83 $\pm$ 0.03

Data are means  $\pm$  SEM.  $n = 4$ –13 per group. \* $P < 0.05$  compared with WT C-C-H; ¶ $P < 0.01$  compared with WT C-C-H; § $P < 0.005$  compared with WT C-C-H; \$ $P < 0.05$  compared with KO H-C-H.

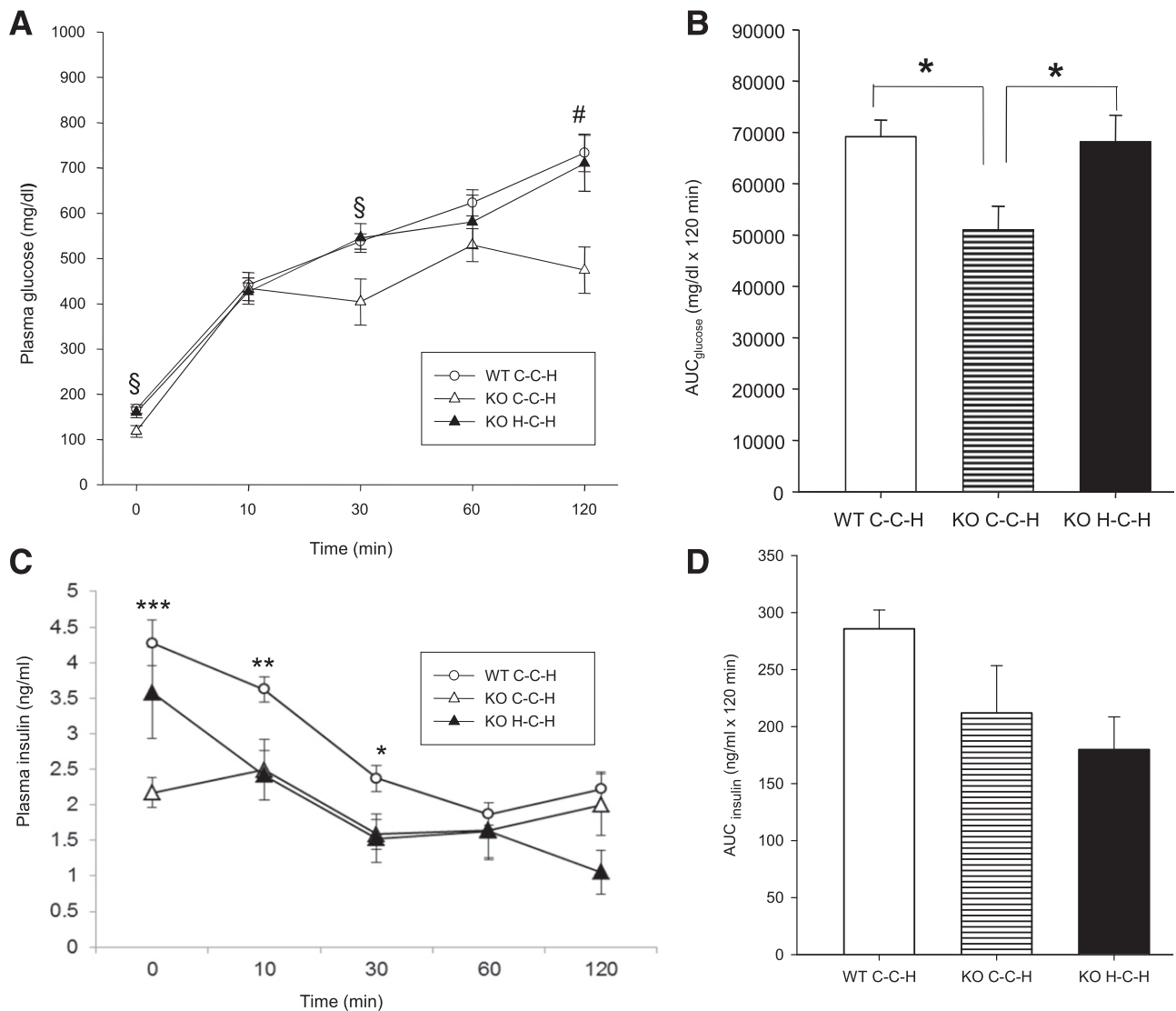


**Figure 3**—GTT at 43 weeks of age (18 weeks on HFD). After an overnight fast, mice received an injection of 2.0 g glucose/kg body wt i.p. **A:** KO C-C-H had significantly improved glucose tolerance compared with WT C-C-H and KO H-C-H. § $P < 0.01$  for KO C-C-H vs. WT C-C-H and  $P < 0.05$  for KO C-C-H vs. KO H-C-H. # $P < 0.05$  for KO C-C-H vs. WT C-C-H and for KO C-C-H vs. KO H-C-H. **B:** KO H-C-H showed higher glucose levels compared with KO C-C-H, although insulin levels were not significantly different. \* $P < 0.05$ . AUC, area under the curve for glucose. **C:** Plasma insulin levels. \* $P < 0.05$ , \*\* $P < 0.01$ , \*\*\* $P < 0.001$  for WT C-C-H vs. KO C-C-H. **D:**  $n = 4$ –13 per group. AUC<sub>insulin</sub>, area under the curve for insulin.

in KO C-C-H compared with WT C-C-H ( $P < 0.01$ ) (Fig. 6A) but was, however, again upregulated in KO H-C-H similar to WT C-C-H. Phosphorylation of hypothalamic Akt at Thr<sup>308</sup> or Ser<sup>473</sup> was not significantly different between the groups (Fig. 6B). For phosphorylation of mTOR at Ser<sup>2448</sup>, a downregulation of 18% ( $P < 0.05$ ) was observed in KO C-C-H compared with WT C-C-H that was again upregulated in KO H-C-H similar to the level of WT C-C-H. A similar regulation was observed for the phosphorylation of S6 at Ser<sup>235/236</sup>.

Gene expression of *Npy* was 1.27-fold upregulated and of *LepR* was 32% downregulated in KO H-C-H compared with KO C-C-H (both  $P < 0.05$ ). There were no significant

changes in expression for other anorexigenic and orexi-genic genes (Supplementary Fig. 2).

#### Altered Promoter Methylation Causes Differential Transcription Factor Binding at the *Ppara* Promoter in Muscle

DNA methylation analyses were performed for the promoter regions of *Ppara*, *Ppargc1a*, *Cpt1b*, and *Cpt1a* in muscle and for the promoter region of *Pik3r1* in hypothalamus. For *Cpt1b*, we identified three CpG sites (CpG<sub>+227/224</sub>, CpG<sub>-72</sub>, and CpG<sub>-202</sub>) that had a loss in DNA methylation in KO C-C-H compared with WT C-C-H (Fig. 7A–C). In KO H-C-H, methylation was again increased as seen in WT C-C-H. These changes in methylation were

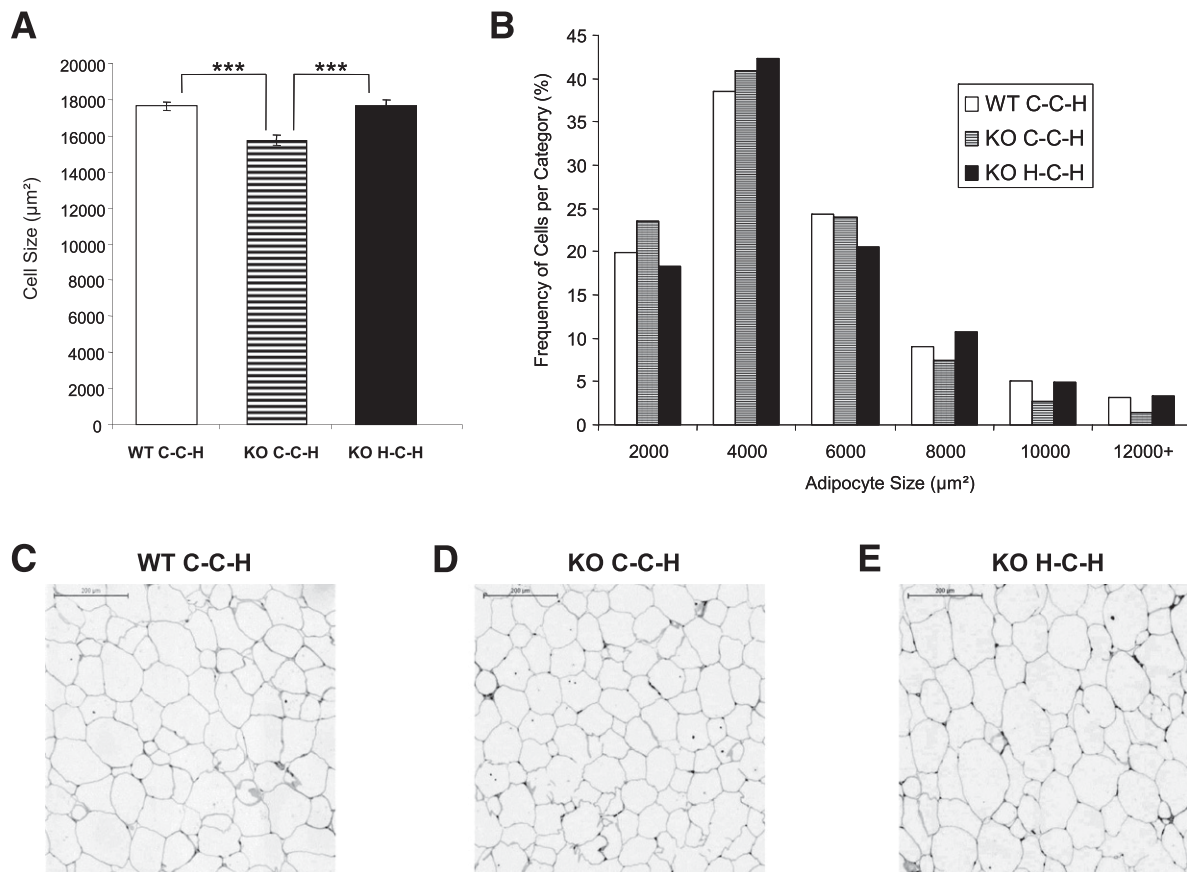


**Figure 4**—Adipocyte cell size was determined in hematoxylin-eosin-stained sections of epididymal white adipose tissue. **A:** KO C-C-H had significantly smaller adipocytes compared with WT C-C-H and KO H-C-H.  $***P < 0.005$ .  $n = 4$ –13 per group. **B:** Histogram of the distribution of cell sizes. Representative image of adipocyte size of WT C-C-H (**C**), KO C-C-H (**D**), and KO H-C-H (**E**).

significantly inversely correlated with gene expression levels of *Cpt1b* ( $r = -0.540$  for CpG<sub>+227/224</sub>,  $P < 0.05$ ;  $r = -0.593$  for CpG<sub>-72</sub>,  $P < 0.05$ ;  $r = -0.629$  for CpG<sub>-202</sub>,  $P < 0.005$ ). For *Ppara*, we identified one CpG site at CpG<sub>-140</sub> (Fig. 7D) that also showed a significant inverse correlation with gene expression levels ( $r = -0.658$ ,  $P < 0.005$ ). We did not see any significant changes in DNA methylation for the promoter of *Ppargc1a* or *Cpt1a* in muscle or of *Pik3r1* in hypothalamus. To identify the biological relevance of DNA methylation at the associated CpG sites, EMSA were performed. We detected methylation-specific binding of transcription factors at the *Ppara* promoter region using nuclear extracts from C2C12 mouse myoblasts in four independent EMSA. We observed additional protein-DNA complex formation at the methylated *Ppara* CpG<sub>-140</sub> site (Fig. 7E). For the other three tested CpG sites, no methylation-specific protein-DNA was detected (Supplementary Figs. 3–5).

## DISCUSSION

This study shows that *Gipr*<sup>-/-</sup> mice are no longer protected from the adverse effects of an HFD in early adulthood when

this diet was applied during IU and L. The phenotypic alterations were evident by increased adiposity, enlarged adipocytes, impaired glucose tolerance, and increased proinflammatory gene expression in adipose tissue in KO H-C-H compared with KO C-C-H mice. KO H-C-H mice behaved similar to WT mice on a normal chow during IU/L and exposed to an HFD later in life. Mechanistically, this phenotype is most likely due to central inhibition of PI3K causing decreased insulin sensitivity in the hypothalamus and to decreased peripheral fatty acid oxidation in skeletal muscle. Moreover, our study suggests that alterations in DNA methylation might be at least partially responsible for the changes in energy consumption. WT mice on HFD during IU/L and reexposed to this diet later in life (WT H-C-H) showed a metabolic phenotype similar to that of WT C-C-H. Results are shown in Supplementary Figs. 6–11.

We did not see a relevant difference in body weight or body fat between KO H-C and KO C-C mice up to the age of 25 weeks. After the HFD was started at the age of 25 weeks, differences for genotypes and maternal diet became evident. KO C-C-H showed significantly lower body weight and total body fat compared with WT C-C-H

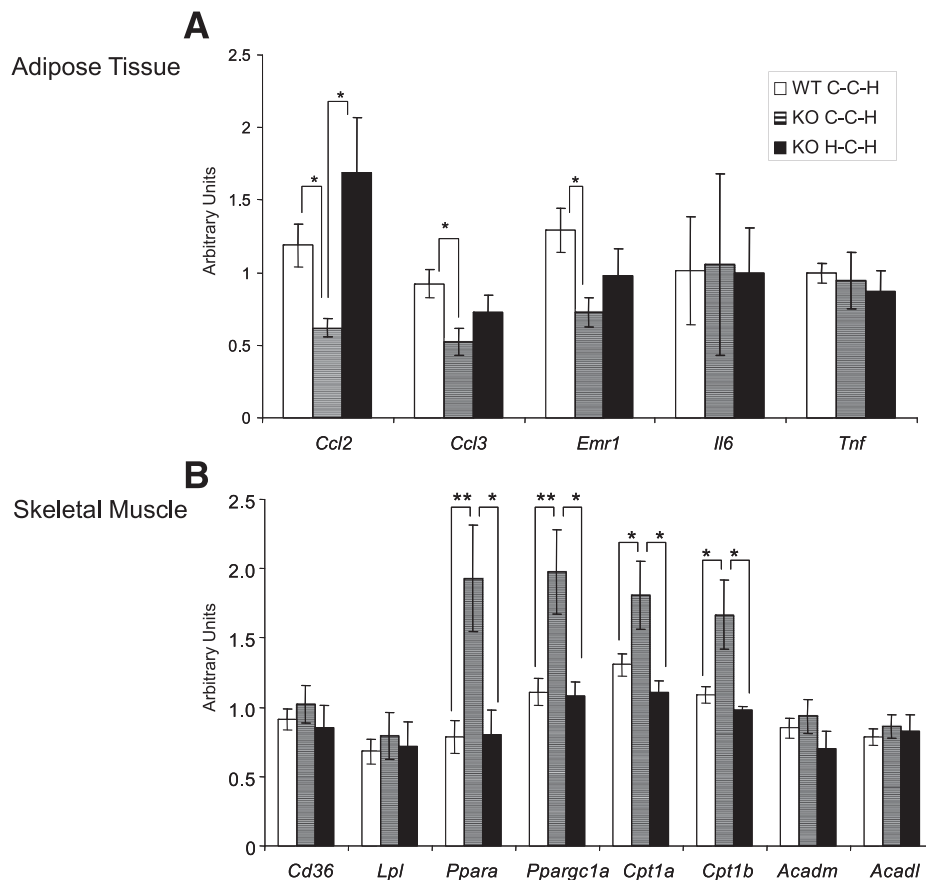


**Figure 5**—Gene expression levels in epididymal adipose tissue (A) and in gastrocnemius muscle (B). \* $P < 0.05$ , \*\* $P < 0.01$ .  $n = 4$ –13 per group. *Acadm*, medium-chain acyl-CoA dehydrogenase; *Acadl*, long-chain acyl-CoA dehydrogenase; *Ccl2*, MCP-1; *Ccl3*, macrophage inflammatory protein-1 $\alpha$ ; *Cd36*, cluster of differentiation 36 fatty acid transporter; *Cpt1a*, carnitine palmitoyltransferase 1 $\alpha$ ; *Cpt1b*, carnitine palmitoyltransferase 1 $\beta$ ; *Emr1*, F4/80, marker of macrophage infiltration; *Il6*, interleukin-6; *Lpl*, lipoprotein lipase; *Ppara*, peroxisome proliferator-activated receptor  $\alpha$ ; *Ppargc1a*, peroxisome proliferator-activated receptor  $\gamma$  coactivator 1 $\alpha$ ; *Tnf*, tumor necrosis factor- $\alpha$ .

as shown previously (5,8). The growth curve of KO H-C-H mice was in between the WT C-C-H and KO C-C-H mice, but KO H-C-H mice had significantly increased total body fat after 6 and 12 weeks upon reexposure to an HFD compared with KO C-C-H mice. We show that even after a time window of 22 weeks on the C diet, *Gipr*<sup>-/-</sup> mice on an HFD during IU/L (“first hit”) are programmed to overreact toward the “second hit” of the HFD compared with *Gipr*<sup>-/-</sup> mice on a C diet during IU/L. This is also reflected by the increased size of adipocytes in KO H-C-H compared with KO C-C-H mice, which is important, since the size of adipocytes is correlated with adipose tissue dysfunction and insulin resistance (22). This strong programming phenomenon was shown recently in a CID1 mouse model (15,22): WT male offspring of dams fed an HFD during IU/L were kept on normal chow after weaning until the age of 25 weeks and then reintroduced to the HFD for 19 weeks. These mice showed higher body weight, larger adipocytes, and reduced glucose tolerance compared with mice exposed to the HFD at 25 weeks of age only.

The GIP signaling pathway is necessary for adipocyte development (23). This might explain why lacking the GIPR protects *Gipr*<sup>-/-</sup> mice from diet-induced obesity (5,24). However, if the HFD appears as a “second hit” later in life, this protection disappears and the fetal programming effect of an HFD overrules the *Gipr*<sup>-/-</sup> phenotype. Nevertheless, there was less weight gain in the KO H-C-H mice than in WT controls suggesting that some protection remained despite fetal programming effects of an HFD. One possible component might relate to the moderate impairment of insulin release in the *Gipr*<sup>-/-</sup> mice, which reduces the obesogenic effect of insulin. It is most likely that KO H-C-H as well as WT C-C-H mice have severe  $\beta$ -cell damage, since serum insulin concentrations were dramatically reduced during the intraperitoneal GTT, whereas KO C-C-H were able to minimally increase insulin release at the beginning of the intraperitoneal GTT.

Obesity is associated with increased gene expression of proinflammatory cytokines or MCP-1 (25). MCP-1 seems

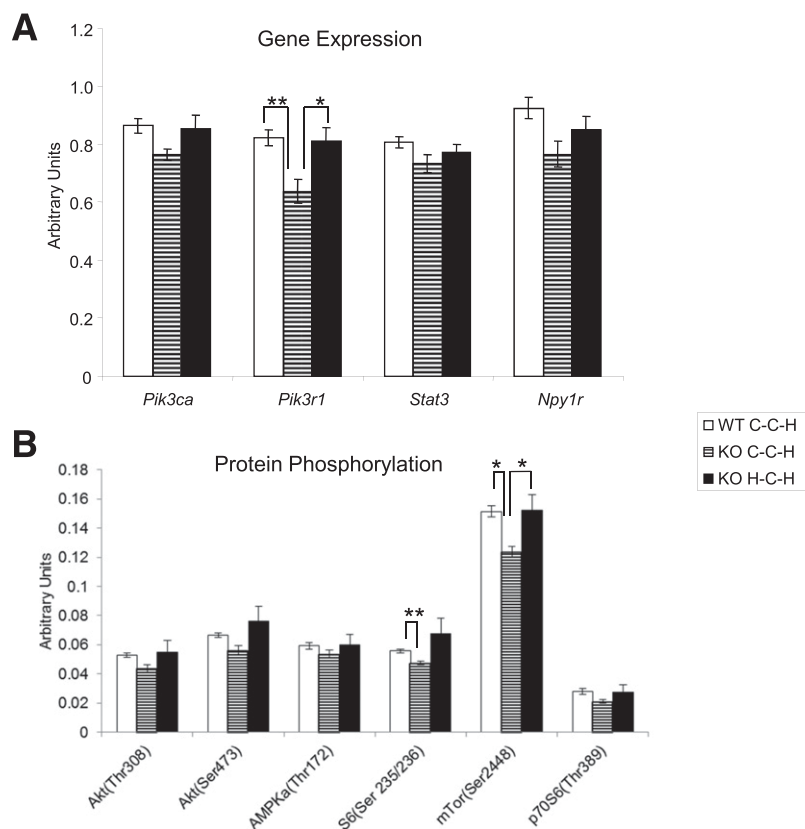


**Figure 6—A:** Gene expression levels in hypothalamus of PI3K catalytic subunit p110 (*Pik3ca*), PI3K regulatory subunit p85 $\alpha$  (*Pik3r1*), signal transducer and activator of transcription 3 (*Stat3*), and neuropeptide Y receptor 1 (*Npy1r*). **B:** Analysis of hypothalamic protein phosphorylation of Akt (Thr<sup>308</sup>), Akt (Ser<sup>473</sup>), AMPKa (Thr<sup>172</sup>), S6 ribosomal protein (Ser<sup>235/236</sup>), mTOR (Ser<sup>2448</sup>), and p70 S6 kinase (Thr<sup>389</sup>). \* $P < 0.05$ , \*\* $P < 0.01$ .  $n = 4$ –13 per group.

to be responsible for macrophage infiltration in adipose tissue (26,27). Macrophage infiltration can be quantified by measuring gene expression of macrophage inflammatory protein 1- $\alpha$  (*Ccl3*) and *Emr1* (28,29). We saw a significant decrease of gene expression of *Ccl2*, *Ccl3*, and *Emr1* in KO C-C-H compared with WT C-C-H. In KO H-C-H, gene expression of *Ccl2* significantly increased, whereas for *Emr1* and *Ccl3* there was a trend for upregulated gene expression in these mice.

Even though the GIPR is absent in skeletal muscle (30,31), genes involved in fatty acid oxidation were significantly upregulated in KO C-C-H compared with WT C-C-H but were downregulated in KO H-C-H. DNA methylation analysis correlated with the transcription data and indicated the induction of epigenetic changes in *Gipr*<sup>-/-</sup> mice in muscle for *Cpt1b* and *Ppara* once they are exposed to an HFD during IU/L. EMSA experiments suggest a functional relevance of the identified *Ppara* CpG<sub>-140</sub> site for transcriptional regulation.

It has been shown that the IU milieu is able to induce epigenetic changes. A study in rats demonstrated that an HFD during IU/L resulted in DNA hypomethylation in liver in young male offspring that seemed to be associated with long-term hepatic dysfunction (32).

Miyawaki et al. (5) reported no differences in food intake between WT and *Gipr*<sup>-/-</sup> mice on an HFD over a period of 4 days. We clearly see an increased cumulative food intake in KO C-C-H compared with WT C-C-H, which matches the observation that *Gipr*<sup>-/-</sup> mice use fat for energy metabolism rather than storing it in adipose tissue (5). This phenomenon was reversed when *Gipr*<sup>-/-</sup> mice were placed on an HFD during IU/L, indicating that GIP physiologically prevents increased energy expenditure in response to increased energy intake as shown earlier (7).

Energy intake is regulated in the hypothalamus, and hypothalamic insulin sensitivity is necessary for balanced food consumption (33). It has been shown that a reduction in the catalytic subunit p85 $\alpha$  of PI3K enhances insulin-stimulated Akt activity (34). It was reported that PI3K subunit p85 $\alpha$  was upregulated in the hypothalamus of mice that were exposed to an HFD throughout IU/L and the first 120 days of life (35). HFD-induced obesity was shown to require activation of PI3K-dependent hypothalamic pathways (36). Our results indicate that KO C-C-H mice have enhanced hypothalamic insulin sensitivity compared with WT C-C-H mice, since we saw a significant reduction of hypothalamic p85 $\alpha$  PI3K gene expression in the former, which correlated with the glucose challenge test. This was reversed in KO H-C-H

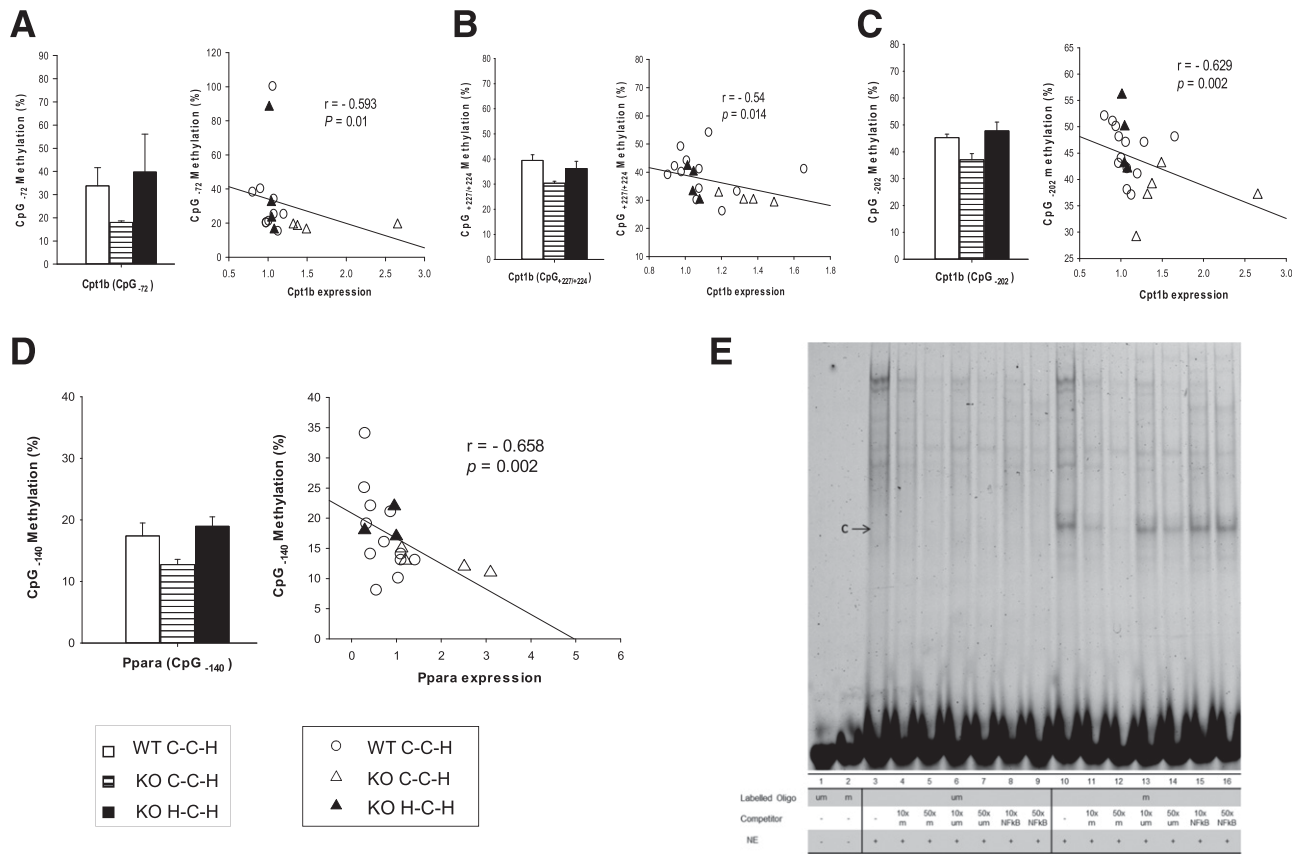


**Figure 7**—DNA methylation of CpG sites of the *Cpt1b* (A–C) and *Ppara* (D) promoter and their correlation with gene expression levels in muscle. DNA methylation of CpG sites is expressed in percent. A negative Spearman correlation coefficient ( $r$ ) indicates inverse correlation between DNA methylation of the CpG site and gene expression. **E**: Methylation-specific formation of a protein–DNA complex in the *Ppara* promoter region in mouse myoblasts. Methylated (m) and unmethylated (um) Cy5-labeled probes carrying the *Ppara* CpG<sub>-140</sub> site were investigated in competition EMSA using C2C12 mouse myoblast nuclear extracts. Lanes 1 and 2 represent oligonucleotides without incubation with nuclear extract. Lanes 3 and 10 represent protein–DNA complex formation at the unmethylated and methylated CpG. In lanes 4, 5, 11, and 12, competition with unlabeled methylated oligonucleotides was performed, whereas in lanes 6, 7, 13, and 14, competition with unlabeled unmethylated oligonucleotides was performed. Specificity was assured by competition experiments with unlabeled nuclear factor- $\kappa$ B (Nf $\kappa$ B) consensus oligonucleotides (lanes 8, 9, 15, and 16). Arrow (C) indicates methylation-specific binding.  $n = 4$ –13 per group.

mice similar to WT C-C-H mice. These results were further supported by increased phosphorylation of the hypothalamic kinase mTOR and S6 protein in the mTOR signaling pathway downstream of Akt. Increased mTOR signaling in the hypothalamus is associated with decreased food intake (37), which was also observed in our study. Thus, central modulation of insulin sensitivity is proposed as a novel mechanism involved in GIP action. However, we could not detect any DNA methylation changes in the p85 $\alpha$  PI3K gene promoter.

In summary, we used the approach of fetal programming by HFD to identify GIP-regulated metabolic pathways that alter hypothalamic insulin sensitivity and the PGC-1 $\alpha$ -driven and peroxisome proliferator-activated receptor  $\alpha$ -driven fat oxidation in skeletal muscle and adipose tissue inflammation.

**Acknowledgments.** The authors thank Elisabeth Meyer, Susann Richter, and Kerstin Weinert, of the German Institute of Human Nutrition, and Nicole

Spada, of the German Research Center for Environmental Health, for excellent technical assistance. Johannes Beckers and Peter Huypens, of the German Research Center for Environmental Health, are acknowledged for valuable comments on mouse genetics. Sonja Kunze, of the German Research Center for Environmental Health, and Elke Rodríguez and Hans-Jörg Baurecht, of the University Hospital, Kiel, Germany, kindly gave advice on methylation analysis. The authors thank Bernard Thorens, of the Department of Physiology and Center for Integrative Genomics, University of Lausanne, Lausanne, Switzerland, for providing the *Gipr*<sup>-/-</sup> mouse model.

**Funding.** This work was supported by a grant from Deutsche Diabetes Gesellschaft to M.K. and a grant from Deutsche Forschungsgemeinschaft (Pf 164/14-2) to A.F.H.P.

**Duality of Interest.** No potential conflicts of interest relevant to this study were reported.

**Author Contributions.** M.K. designed experiments, researched data, wrote and edited the manuscript, and obtained funding supporting the research. F.K.-N. researched data and wrote and edited the manuscript. F.I. designed experiments and researched data. B.N., A.K., E.R., and H.G. designed experiments, researched data, and wrote and edited the manuscript. T.d.I.H.G. and M.A.O. analyzed data. A.F.H.P. designed experiments, wrote and edited the

manuscript, and obtained funding supporting the research. A.F.H.P. is the guarantor of this work and, as such, had full access to all the data in the study and takes responsibility for the integrity of the data and the accuracy of the data analysis.

## References

1. Baggio LL, Drucker DJ. Biology of incretins: GLP-1 and GIP. *Gastroenterology* 2007;132:2131–2157
2. Yip RG, Wolfe MM. GIP biology and fat metabolism. *Life Sci* 2000;66:91–103
3. Kim SJ, Nian C, McIntosh CH. Activation of lipoprotein lipase by glucose-dependent insulinotropic polypeptide in adipocytes. A role for a protein kinase B, LKB1, and AMP-activated protein kinase cascade. *J Biol Chem* 2007;282:8557–8567
4. Gögebakan Ö, Andres J, Biedasek K, et al. Glucose-dependent insulinotropic polypeptide reduces fat-specific expression and activity of 11 $\beta$ -hydroxysteroid dehydrogenase type 1 and inhibits release of free fatty acids. *Diabetes* 2012;61:292–300
5. Miyawaki K, Yamada Y, Ban N, et al. Inhibition of gastric inhibitory polypeptide signaling prevents obesity. *Nat Med* 2002;8:738–742
6. Isken F, Pfeiffer AF, Nogueiras R, et al. Deficiency of glucose-dependent insulinotropic polypeptide receptor prevents ovariectomy-induced obesity in mice. *Am J Physiol Endocrinol Metab* 2008;295:E350–E355
7. Isken F, Weickert MO, Tschöp MH, et al. Metabolic effects of diets differing in glycaemic index depend on age and endogenous glucose-dependent insulinotropic polypeptide in mice. *Diabetologia* 2009;52:2159–2168
8. Hansotia T, Maida A, Flock G, et al. Extrapancreatic incretin receptors modulate glucose homeostasis, body weight, and energy expenditure. *J Clin Invest* 2007;117:143–152
9. Warner MJ, Ozanne SE. Mechanisms involved in the developmental programming of adulthood disease. *Biochem J* 2010;427:333–347
10. Alfaradhi MZ, Ozanne SE. Developmental programming in response to maternal overnutrition. *Front Genet* 2011;2:27
11. Swenne I, Crace CJ, Milner RD. Persistent impairment of insulin secretory response to glucose in adult rats after limited period of protein-calorie malnutrition early in life. *Diabetes* 1987;36:454–458
12. Armitage JA, Taylor PD, Poston L. Experimental models of developmental programming: consequences of exposure to an energy rich diet during development. *J Physiol* 2005;565:3–8
13. Samuelsson AM, Matthews PA, Argenton M, et al. Diet-induced obesity in female mice leads to offspring hyperphagia, adiposity, hypertension, and insulin resistance: a novel murine model of developmental programming. *Hypertension* 2008;51:383–392
14. Oben JA, Mouralidarane A, Samuelsson AM, et al. Maternal obesity during pregnancy and lactation programs the development of offspring non-alcoholic fatty liver disease in mice. *J Hepatol* 2010;52:913–920
15. Kruse M, Seki Y, Vuguin PM, et al. High-fat intake during pregnancy and lactation exacerbates high-fat diet-induced complications in male offspring in mice. *Endocrinology* 2013;154:3565–3576
16. Burdge GC, Hanson MA, Slater-Jefferies JL, Lillycrop KA. Epigenetic regulation of transcription: a mechanism for inducing variations in phenotype (fetal programming) by differences in nutrition during early life? *Br J Nutr* 2007;97:1036–1046
17. Ristow M, Mulder H, Pomplun D, et al. Frataxin deficiency in pancreatic islets causes diabetes due to loss of beta cell mass. *J Clin Invest* 2003;112:527–534
18. Hartil K, Vuguin PM, Kruse M, et al. Maternal substrate utilization programs the development of the metabolic syndrome in male mice exposed to high fat in utero. *Pediatr Res* 2009;66:368–373
19. Ranalletta M, Du XQ, Seki Y, et al. Hepatic response to restoration of GLUT4 in skeletal muscle of GLUT4 null mice. *Am J Physiol Endocrinol Metab* 2007;293:E1178–E1187
20. Ehrlich M, Nelson MR, Stanssens P, et al. Quantitative high-throughput analysis of DNA methylation patterns by base-specific cleavage and mass spectrometry. *Proc Natl Acad Sci U S A* 2005;102:15785–15790
21. Zeilinger S, Kühnel B, Klopp N, et al. Tobacco smoking leads to extensive genome-wide changes in DNA methylation. *PLoS One* 2013;8:e63812
22. Goossens GH. The role of adipose tissue dysfunction in the pathogenesis of obesity-related insulin resistance. *Physiol Behav* 2008;94:206–218
23. Song DH, Getty-Kaushik L, Tseng E, Simon J, Corkey BE, Wolfe MM. Glucose-dependent insulinotropic polypeptide enhances adipocyte development and glucose uptake in part through Akt activation. *Gastroenterology* 2007;133:1796–1805
24. Naitoh R, Miyawaki K, Harada N, et al. Inhibition of GIP signaling modulates adiponectin levels under high-fat diet in mice. *Biochem Biophys Res Commun* 2008;376:21–25
25. Trayhurn P. Endocrine and signalling role of adipose tissue: new perspectives on fat. *Acta Physiol Scand* 2005;184:285–293
26. Weisberg SP, McCann D, Desai M, Rosenbaum M, Leibel RL, Ferrante AW Jr. Obesity is associated with macrophage accumulation in adipose tissue. *J Clin Invest* 2003;112:1796–1808
27. Oh DY, Morinaga H, Talukdar S, Bae EJ, Olefsky JM, Oh da Y. Increased macrophage migration into adipose tissue in obese mice. *Diabetes* 2012;61:346–354
28. Sell H, Eckel J. Chemotactic cytokines, obesity and type 2 diabetes: in vivo and in vitro evidence for a possible causal correlation? *Proc Nutr Soc* 2009;68:378–384
29. Rausch ME, Weisberg S, Vardhana P, Tortorello DV. Obesity in C57BL/6J mice is characterized by adipose tissue hypoxia and cytotoxic T-cell infiltration. *Int J Obes* 2008;32:451–463
30. Usdin TB, Mezey E, Button DC, Brownstein MJ, Bonner TI. Gastric inhibitory polypeptide receptor, a member of the secretin-vasoactive intestinal peptide receptor family, is widely distributed in peripheral organs and the brain. *Endocrinology* 1993;133:2861–2870
31. Zhou H, Yamada Y, Tsukiyama K, et al. Gastric inhibitory polypeptide modulates adiposity and fat oxidation under diminished insulin action. *Biochem Biophys Res Commun* 2005;335:937–942
32. Dudley KJ, Sloboda DM, Connor KL, Beltrand J, Vickers MH. Offspring of mothers fed a high fat diet display hepatic cell cycle inhibition and associated changes in gene expression and DNA methylation. *PLoS One* 2011;6:e21662
33. Sharma MD, Garber AJ, Farmer JA. Role of insulin signaling in maintaining energy homeostasis. *Endocr Pract* 2008;14:373–380
34. Mauvais-Jarvis F, Ueki K, Fruman DA, et al. Reduced expression of the murine p85alpha subunit of phosphoinositide 3-kinase improves insulin signaling and ameliorates diabetes. *J Clin Invest* 2002;109:141–149
35. Page KC, Malik RE, Ripple JA, Anday EK. Maternal and postweaning diet interaction alters hypothalamic gene expression and modulates response to a high-fat diet in male offspring. *Am J Physiol Regul Integr Comp Physiol* 2009;297:R1049–R1057
36. Klöckener T, Hess S, Belgardt BF, et al. High-fat feeding promotes obesity via insulin receptor/PI3K-dependent inhibition of SF-1 VMH neurons. *Nat Neurosci* 2011;14:911–918
37. Cota D, Proulx K, Smith KA, et al. Hypothalamic mTOR signaling regulates food intake. *Science* 2006;312:927–930